

Optimal Design of a Boost-type DC-DC Converter for PV Power-Supplied Wireless Sensor Networks

Ioannis Mandourarakis, Eftichios Koutroulis
School of Electronic and Computer Engineering
Technical University of Crete, Chania, Greece
i.mandourarakis@gmail.com, efkout@electronics.tuc.gr

Abstract—*Wireless Sensor Networks (WSNs) are widely installed during the last years for monitoring multiple parameters of interest over distributed areas in the environment, buildings and industries. The WSN nodes are frequently installed in geographically remote areas. Thus, they are power-supplied by renewable energy sources and a DC-DC power converter is employed for interfacing the generated energy to a battery bank and the electric load of the WSN node. In this paper, an optimization method is presented for performing circuit-level optimization of a Photovoltaic (PV) power-supplied Boost-type DC-DC power converter, which is employed in a WSN node. Using the proposed technique enables to calculate the optimal switching frequency and values of the components comprising the circuit of the DC-DC converter, such that either the power loss at nominal output power, or the total power loss during the year, or the Levelized Cost Of the Electricity generated (LCOE), are alternatively minimized. The design optimization and experimental results demonstrate the features of the proposed technique and confirm the performance superiority of the DC-DC converters, which are designed using the proposed method, compared to the non-optimized DC-DC converter structures.*

Keywords—*DC-DC converter, optimization, efficiency, genetic algorithms*

I. INTRODUCTION

The installation of Wireless Sensor Networks (WSNs) has been increased during the last years, since they enable the measurement of multiple parameters of interest (e.g. meteorological conditions, operational parameters in buildings and industrial environments etc.) over distributed areas [1]. The WSN nodes are frequently installed in geographically remote sites, where there is lack of electricity. Thus, the WSN nodes, comprising sensors and data-acquisition devices, are power-supplied by Renewable Energy Sources (RES, e.g. photovoltaics, wind-generators etc.) and the RES-generated power is interfaced through a DC-DC converter to a battery bank and the electric load (e.g. data-acquisition devices, wireless transmitters etc.).

During the design of a DC-DC converter, various operational parameters must be considered in order to ensure that the desired performance is achieved, such as the power conversion efficiency, power density, cost, reliability etc. The designer must also perform the appropriate decisions in order to address possible issues that may arise in special circumstances where the thermal flow, temperature distribution and electromagnetic interference (EMI) deserve extra care. An example of thermal and EMI modeling and analysis is given

in [2]. In [3], the trade-off between accuracy and computation time is explored for producing a dedicated optimization tool, by focusing on the converter performance in terms of the power conversion efficiency, EMI and thermal profile.

Optimization techniques have been widely applied for improving the performance of automotive control systems [4, 5], reactive power flow [6-8], DC/AC inverters of Photovoltaic (PV) systems [9-11], etc. Regarding component sizing of DC-DC converters for power loss optimization, only a few studies have taken place with [4, 5, 12, 13] mainly focusing on the minimization of the volume and cost of an automotive Buck-type DC-DC converter and [14] focusing on the low cost of the prototypes.

The DC-DC converters employed in PV power processing systems, such as those implemented for power-supplying the nodes of a WSN, are required to operate under continuously variable DC input-power conditions. Thus, they should be able to optimally exploit the available RES energy for minimizing the total cost of the required RES and energy-storage units, as well as for maximizing the reliability of the overall power-supply system in order to ensure an uninterrupted operation of the WSN node. In this paper, an optimization method is presented for optimally designing the circuit of a Boost-type DC-DC power converter employed in the energy-processing system of a WSN node, which is power-supplied by a PV source. The target of the proposed method is to derive the optimal switching frequency and values of the components comprising the circuit of a PV power-supplied Boost-type converter, which result in optimal operation in terms of performance metrics such as the power loss at maximum output power, total power loss during the year and Levelized Cost Of the Electricity generated (LCOE). The proposed technique also takes into account the stochastic variability of the meteorological conditions at the installation site, which affects the corresponding RES energy production. To the authors' knowledge, no study has yet been carried out investigating the optimization of the circuit-level design of a PV power-supplied DC-DC converter, by also considering the converter power-loss profile during the year, as well as its manufacturing cost. The simulation and experimental results, which are presented in the paper, verify that the optimized DC-DC converters, which are designed using the proposed technique, exhibit superior performance compared to the

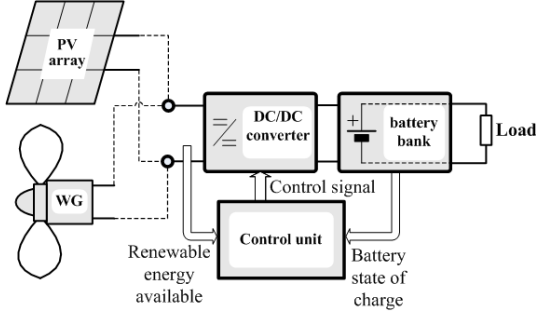


Fig. 1. A block diagram of the WSN node energy management system.

non-optimized DC-DC converters, when both operate under the same meteorological conditions.

II. DC-DC CONVERTER MODELING

A block diagram of the power processing system of a WSN node is shown in Fig. 1. To achieve energy independence, the WSN node is powered by one or more PV modules. Alternatively, a wind turbine (WT) may be used, depending on the availability of solar and wind power in the field of installation. A battery bank is used to store the surplus of PV-generated energy and a control unit regulates the DC-DC converter for implementing the Maximum Power Point Tracking (MPPT) and battery-charging operations [15, 16]. The output voltage of the battery load is considered to fluctuate between 11 V and 14.8 V in normal operating conditions. In this study, the DC-DC converter is designed to operate in the Continuous Conduction Mode (CCM). The equivalent circuit of the Boost-type is depicted in Fig. 2. The parasitic components, which affect the power loss of the DC-DC converter (i.e. $r_{c,in}$, r_L , r_{ds} etc.) are also included in that circuit.

Multiple power MOSFETs may be connected in parallel, depending on the power-loss and manufacturing cost requirements and they are typically controlled by the same control signal generated by a gate-drive circuit, such that they operate concurrently according to the Pulse Width Modulation (PWM) technique. The components playing a dominant role in the power losses and cost of the circuit are the MOSFET switch(es), the power diode, the inductor and the output capacitor. Their electrical characteristics, together with the value of the switching frequency of the DC-DC converter PWM control signal, shape the power-consumption behavior of the overall Boost-type DC-DC converter.

The total power loss of the DC-DC power converter is given by the following equation:

$$P_L = P_{MOSFET} + P_{Diode} + P_{Inductor} + P_{Cout} + P_C \quad (1)$$

where P_{MOSFET} , P_{Diode} , $P_{Inductor}$, P_{Cout} and P_C are the power loss of the power MOSFET(s), diode, inductor and output capacitor, respectively, of the DC-DC converter, while P_C is the total power loss of the input capacitor and control unit, which have been assumed to be constant.

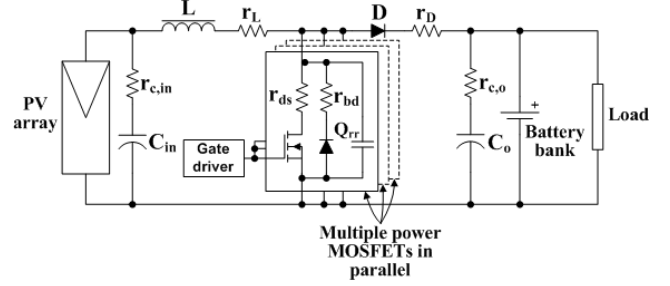


Fig. 2. The equivalent circuit of a Boost-type DC-DC converter.

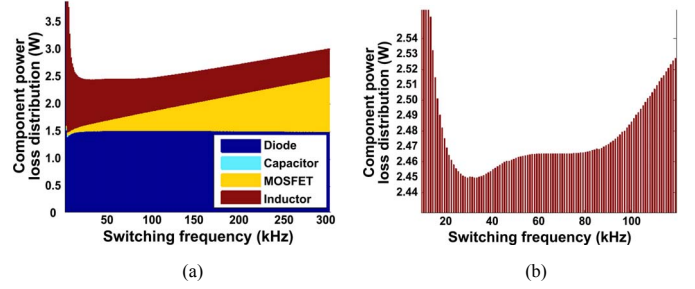


Fig. 3. (a) Power loss distribution among the dominant (in terms of power-loss) components of a Boost-type DC-DC converter for various switching-frequency values and (b) A zoomed-in part of the plot in (a), demonstrating the fluctuation of the overall power loss and its local minimum at 31kHz.

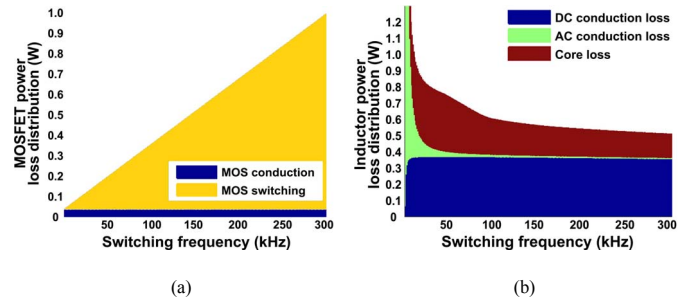


Fig. 4. Distribution of power losses in individual components of the Boost-type DC-DC converter: (a) power MOSFET and (b) inductor.

The analytical equations which are required for calculating the conduction and switching semiconductor losses of the power MOSFET(s) and diode have been composed by the information available in [17-19]. Similarly, the copper and core losses of the inductor are calculated according to [19-22]. The operational parameters of the DC-DC converter components, which are applied in (1), are extracted from the information available in the datasheets provided by the components manufacturers by using the ‘‘Piecewise Cubic Hermite Interpolating Polynomial’’ of the Mathworks MATLAB platform.

In order to investigate its performance in terms of the total power loss, a Boost-type DC-DC power converter has been considered comprising a 100 μ H inductance and operating with a 48 W input power at 6.5 V and 12 V DC input and output voltage levels, respectively. The output current and voltage ripple factors were constrained to be less than 10%. The distribution of total power loss among the dominant (in terms of power loss) components of the DC-DC converter for

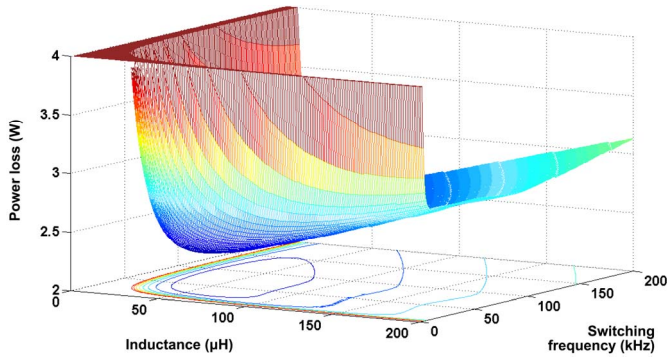


Fig. 5. Total power loss of the DC-DC converter for various values of switching frequency and inductance.

various switching-frequency values are depicted in Fig. 3. The capacitor power loss is much lower than that of the rest of the DC-DC converter components. The total power loss of the DC-DC converter exhibits a local minimum at 31 kHz. As demonstrated next, during the design process of a DC-DC converter, constraints are imposed by the designer, which shift the optimum operating point from that local minimum point.

The distribution of the power losses in the MOSFET switch and power inductor is illustrated in Fig. 4, revealing the scale of influence of each type of losses in the respective components. By observing the simulation results of Fig. 4 it becomes evident that, at the power level under consideration, the MOSFET power loss is highly affected by its switching losses, while the inductor power loss fluctuations are mostly dependent upon its core loss distribution, changing its shape throughout the entire frequency spectrum.

A plot of the total power loss of the DC-DC converter for various values of switching frequency and inductance is depicted in Fig. 5. Additional plots, which were generated for up to four MOSFETs connected in parallel, indicated that the shape of the surface shown in Fig. 5 preserves its monotony while the neighbourhood of the global minimum is moving towards higher losses of about 3% for each additional power MOSFET connected in parallel.

The simulation results presented above indicate that due to the non-linear nature of the total power loss function, the use of an efficient optimization tool such as Genetic Algorithms (GAs) is required for deriving the optimal values of the components and switching frequency, which minimize the total power loss of the DC-DC converter.

III. DC-DC CONVERTER CIRCUIT DESIGN OPTIMIZATION

In order to optimally exploit the power generation capacity of the installed PV source, the power processing interface must be designed so that the generated power is efficiently interfaced to the battery bank. This is achieved by applying an optimization method for designing the circuit of the DC-DC converter, as analyzed in the following.

The target of the proposed, circuit-level optimization method is to derive the optimal switching frequency and values of the components comprising the DC-DC converter, so

that the desired performance metric of the power converter is optimized. The design variables considered in the optimization process are the switching frequency, f_s , the number of power MOSFETs connected in parallel, MF_{Count} , the inductance, L and the output capacitance C_{out} . The optimization process is performed for deriving the optimal values of three alternative performance metrics, which correspond to alternative objective functions of the optimization process. The first one maximizes the power converter efficiency under nominal output power conditions. The power conversion efficiency, η , is given by the following equation:

$$\eta = \frac{P_o}{P_{PV}} = \frac{P_o}{P_o + P_L} \quad (2)$$

where P_{PV} is the power produced by the PV source under MPPT conditions and P_o is the output power of the DC-DC converter.

In order to achieve this target, the minimum value of P_L is calculated using (1) under the condition that the value of P_o is equal to the nominal output power of the DC-DC converter.

The second optimization objective is to minimize the total energy loss of the DC-DC converter during the year, which is given by the following equation:

$$E_{L,tot} = \sum_{i=1}^{8760} P_{L,i} \cdot \Delta t \quad (3)$$

where $P_{L,i}$ is the total power loss of the DC-DC converter at hour i ($1 \leq i \leq 8760$) and Δt is the time-step which has been set equal to 1 h.

The third alternative target of the proposed optimization process is to minimize the Levelized Cost Of the Electricity generated ($LCOE$), which is calculated as follows:

$$LCOE = \frac{C_m}{E_{tot}} = \frac{C_m}{\sum_{i=1}^{8760} (P_{pv,i} - P_{L,i}) \cdot \Delta t} \quad (4)$$

where C_m (€) is the total manufacturing cost of the DC-DC converter, E_{tot} is the total energy transferred to the battery bank during the year and $P_{pv,i}$ is the output power of the PV source at hour i ($1 \leq i \leq 8760$).

The value of C_m in (4) is equal to the sum of the prices of the individual components comprising the DC-DC converter. The output current of the DC-DC converter, I_o , which is required for deriving the value of P_L in (1)-(4), is calculated for each value of PV-generated power during the year by numerically solving, using a properly developed software program, the following power-balance equation:

$$P_{pv} = P_L + V_o \cdot I_o \quad (5)$$

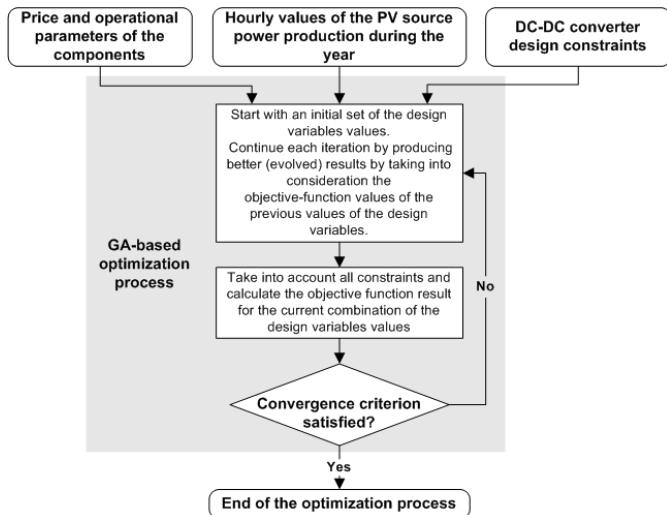


Fig. 6. A flowchart of the proposed circuit-level optimization process using GAs.

where P_{pv} is the power produced by the PV source and V_o is the output voltage of the DC-DC converter.

A flowchart of the proposed optimization process is illustrated in Fig. 6. Initially, the designer specifies the price and operational parameters of the components which are used to build the DC-DC converter, the hourly values of the PV source power production during the year, as well as the desired constraints which must be considered during the DC-DC converter design process, such as the maximum permissible switching frequency and output voltage/current ripple factors. Then, the values of the design variables f_s , MF_{Count} , L and C_{out} resulting in the optimization of objective functions (2)-(4) are calculated using GAs, which operate as search heuristics, mimicking the process of natural selection [23]. GAs belong in the larger class of evolutionary algorithms whose functions are inspired by techniques such as inheritance, mutation, selection and crossover. They serve as excellent tools when it comes to produce good estimations about non-linear or stochastic optimization problems. During the execution of the proposed optimization process, multiple alternative values of the design variables are produced by GAs and the desired objective function is evaluated [i.e. one of (2)-(4)] for each one of them. In case that any combination of f_s , MF_{Count} , L and C_{out} results in a violation of the DC-DC converter design constraints, then it is not further considered as a potentially optimal solution. This process is repeated until a predefined number of similar iterations have been executed.

IV. OPTIMIZATION RESULTS

In order to investigate the features of the proposed optimization methodology, the algorithm shown in Fig. 6 was initially implemented by developing a software program, which operates under the MATLAB platform. The optimal design of a 50 W Boost-type DC-DC converter, which is fed by two PV modules with a 20 W power rating each under Standard Test Conditions (STC), installed in the area of Chania (Greece), was then performed using that optimization

TABLE I. THE OPTIMAL VALUES OF THE DESIGN VARIABLES.

Design Variable	Objective function		
	Power loss at maximum output power	Total energy loss during the year	LCOE
MF_{Count}	1	1	1
L	95 μ H	122 μ H	77 μ H
C_{out}	3.0 mF	3.0 mF	0.032 mF
f_s	128.4 kHz	153.9 kHz	242.3 kHz

TABLE II. THE DC-DC CONVERTER PERFORMANCE FOR THE ALTERNATIVE OBJECTIVE FUNCTIONS, WHICH HAVE BEEN EMPLOYED IN THE PROPOSED OPTIMIZATION PROCESS.

Metric	Objective function		
	Minimum power loss at maximum output power	Minimum total energy loss during the year	Minimum LCOE
Efficiency (%)	93.0 %	92.3 %	92.0 %
Total energy loss during the year (kWh)	5.784 kWh	5.670 kWh	6.015 kWh
LCOE (€/Wh)	0.136 €/Wh	0.140 €/Wh	0.119 €/Wh

tool. For the LCOE calculations in (4), the prices of the DC-DC converter circuit components in the international market were considered.

The resulting optimal values of the design variables for the three alternative objective functions described in Section III, are presented in Table I. It is observed that a different set of optimal values is derived in each case, since, in contrast to the efficiency at nominal output power, the annual energy loss and LCOE metrics incorporate the impact of the continuously variable input power of the PV power-supplied DC-DC converter during the year. Also, the LCOE metric additionally takes into account the DC-DC converter manufacturing cost.

The DC-DC converter performance for the alternative objective functions, which have been employed in the proposed optimization process, is illustrated in Table II. For each objective function optimized, the resulting set of optimal values of design variables (i.e. Table III) has been applied for calculating the values of the other two objective functions and the corresponding results are also presented in Table II. In case that the DC-DC converter is optimized for achieving minimum power loss at nominal output power, then the resulting efficiency is higher by 0.7-1.0 % than the efficiency obtained when applying the $E_{L,tot}$ and LCOE objective functions [given by (3) and (4), respectively]. Similarly, the minimum total energy loss is lower by 2.0-5.7 % than the annual energy loss resulting when optimizing the power loss at maximum power and LCOE, respectively. The optimal LCOE value is lower by 8.8-15.0 % than the LCOE of the DC-DC converters which have been optimized for minimum power loss (either at maximum output power, or annual power loss).

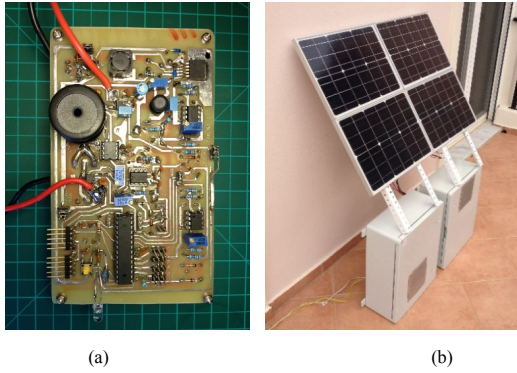


Fig. 7. Picture (a) on the left shows the experimental prototype of a PV-powered Boost-type DC-DC converter, which has been optimally designed using the proposed method. Picture (b) on the right shows the workbench setup for the performance comparison of the optimized and non-optimized DC-DC converters.

The proposed GA-based optimization process was accomplished by the developed software program in about 40 minutes, with a precision of less than 1 %.

V. EXPERIMENTAL RESULTS

In order to experimentally evaluate the performance of the DC-DC converters, which are optimally designed using the proposed methodology, two identical prototype circuits were constructed using off-the-shelf components. The first one was developed by applying the optimal values of the design variables f_s , MF_{Count} , L and C_{out} , which have been derived by executing the proposed design optimization procedure for minimizing the power loss at maximum output power, while the second one was constructed without applying a design optimization process. The difference between these two DC-DC converters were the inductance and switching frequency values which were employed. The optimized DC-DC converter was built using a 100 μ H inductor and a switching frequency of 128 kHz, so that the corresponding optimization results shown in Table I are approximated using the closest available values of the components. In contrast, a 390 μ H inductor and a 97 kHz switching frequency were employed in the non-optimized DC-DC converter. The voltage and current ripple constraints were also satisfied by the non-optimized DC-DC converter. The experimental prototype of a PV power-supplied Boost-type DC-DC converter, which has been optimally designed using the proposed method, is depicted in Fig. 7(a). Each prototype DC-DC converter was then connected to a different battery bank comprising lead-acid batteries, which were all charged at the same voltage point of 12.41 V (measured under open-circuit conditions) and also power-supplying the same constant load of an Alix 3d3 PC Engine, comprising the WSN node load, which was kept in the power-on self-test mode of operation. Also, both DC-DC converters were receiving power from exactly the same type of solar panels standing side-by-side and facing towards the same direction [Fig. 7(b)]. In order to maximize the power produced by the PV modules under the continuously varying solar irradiation and ambient temperature conditions at the installation site, the control units of the DC-DC converters were programmed to execute a ‘‘Perturbation and

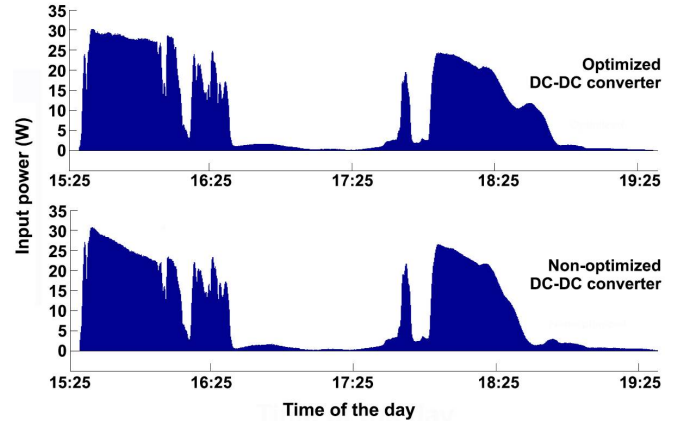


Fig. 8. The experimentally measured time-series of the power, which was produced by the PV sources of the optimized and non-optimized DC-DC converters, respectively, under MPPT conditions.

TABLE III. COMPARISON OF THE OPTIMIZED AND NON-OPTIMIZED DC-DC CONVERTERS IN TERMS OF THE ENERGY CONVERSION EFFICIENCY.

	<i>Parameter</i>	<i>Value</i>
<i>Optimized DC-DC converter</i>	E_{PV} (Wh)	19.86
	E_o (Wh)	13.82
	n_e (%)	69.6
<i>Non-optimized DC-DC converter</i>	E_{PV} (Wh)	19.73
	E_o (Wh)	13.02
	n_e (%)	66.0

Observation’’ Maximum Power Point Tracking (MPPT) process [24]. The two WSN nodes were installed to operate simultaneously for a time period of four hours. The experimentally measured time-series of the power, which was produced by the PV sources of the optimized and non-optimized DC-DC converters, respectively, are shown in Fig. 8. The energy production is substantially reduced during 16:33-17:45 due to sky clouding. The total energy produced by each PV array (E_{PV}) as well as the total energy transferred to each battery bank (E_o) respectively, during that test period, are presented in Table III. In order to compare the performance of the optimized and non-optimized DC-DC converters, without being affected by the deviation of the operational characteristics of the solar panels and batteries which were used in each of the two experimental prototypes, the normalized energy conversion efficiency has been calculated as follows:

$$n_e = \frac{E_o}{E_{PV}} \quad (6)$$

As shown in Table III, the normalized energy conversion efficiency of the optimized DC-DC converter circuit is higher than that of the non-optimized one by 3.6 %, thus demonstrating the superiority offered by the proposed design optimization method. The n_e metric is affected by the performance of the DC-DC converter over a wide operating power range, thus it is lower than the value of power

conversion efficiency at maximum output power which has been reported in Table II, due to the drop of efficiency at low power levels.

VI. CONCLUSION

WSNs are widely installed for monitoring multiple parameters of interest over distributed areas in the environment, buildings and industries. Since they are frequently installed in geographically remote areas, the WSN nodes are power-supplied by RES. Thus, a DC-DC power converter is employed for interfacing the generated energy to a battery bank and the electric load of the WSN node. In this paper, an optimization method has been presented for performing circuit-level optimization of a PV power-supplied Boost-type DC-DC power converter, which is employed in a WSN node. Using the proposed technique enables to calculate the optimal switching frequency and values of the components comprising the circuit of the DC-DC converter, such that either the power loss at nominal output power, or the total power loss during the year, or the LCOE, are alternatively minimized. Design optimization and experimental results have been presented, which demonstrate the features of the proposed technique and confirm the performance superiority of the DC-DC converters designed using the proposed method, compared to the non-optimized DC-DC converter structures. Future work includes the long-term experimental testing of the optimized DC-DC converters, in order to evaluate their performance in terms of annual energy loss and energy production during the year.

ACKNOWLEDGMENT

This work was supported by the SYN11-6-925 AquaNet project, which is executed within the framework of the "Cooperation 2011" program of the Greek General Secretariat for Research & Technology (GSRT), funded through European Union and national funds. The authors thank "Georgios Lontas & Co. E.E." (Katerini, Greece) for their contribution in the development of the experimental prototype systems, as well as the administration and research/technical personnel of the Telecommunication Systems Research Institute (Technical University of Crete, Greece) for their assistance in conducting this research.

REFERENCES

1. K. Shafiqullah, K.P. Al-Saki, and A.A. Nabil, "Wireless Sensor Networks - Current Status and Future Trends," CRC Press, 2012.
2. F. Wang, W. Shen, D. Boroyevich, S. Ragon, V. Stefanovic and M. Arpilliere, "Design optimization of industrial motor drive power stage using Genetic Algorithms," CES/IEEE 5th International Power Electronics and Motion Control Conference (IPEMC), vol. 1, pp. 1-5, 2006.
3. C. Larouci, J. P. Didier, A. Aldebert, O. Bouquet, A. Prost and J. Vauchel, "Optimal design of a synchronous DC-DC converter using analytical models and a dedicated optimization tool," 29th Annual Conference of the IEEE Industrial Electronics Society (IECON), vol. 2, pp. 1623-1628, 2003.
4. H. Helali, D. Bergogne, H. Morel and J. B. H. Slama, "Power converter design methodology: uses of multiple objective techniques for optimization of a (42/14V) buck converter," 4th International Conference on Integrated Power Systems (CIPS), pp.1-5, 2006.
5. K. Ejjabraoui, C. Larouci, P. Lefranc and C. Marchand, "A new pre-sizing approach of DC-DC converters, application to a boost

- converter for the automotive domain," 35th Annual Conference of the IEEE Industrial Electronics Society (IECON), pp. 3767-3772, 2009.
6. X. Ma and R. L. Liu, "Reactive power optimization in power system based on improved niche genetic algorithm," International Conference on Computer Design and Applications (ICCD), vol. 3, pp. 413-416, 2010.
7. K. Rayudu, A. Jayalaxmi, G. Yesuratnam and Y. D. Kumar, "Multi objective comparison of GA and LP techniques for generator reactive power optimization," IEEE 5th Power India Conference, pp.1-5, 2012.
8. R. Lukowski and K. Wilkosz, "Optimization of reactive power flow in a power system for different criteria: stability problems," 8th International Symposium on Advanced Topics in Electrical Engineering (ATEE), pp. 1-6, 2013.
9. S. Chen, P. Li, D. Brady and B. Lehman, "Determining the optimum grid-connected photovoltaic inverter size," Solar Energy, vol. 87, pp. 96-116, 2013.
10. J. Luoma, J. Kleissl and K. Murray, "Optimal inverter sizing considering cloud enhancement," Solar Energy, vol. 86, pp. 421-429, 2012.
11. E. Koutroulis and F. Blaabjerg, "Design optimization of transformerless grid-connected PV inverters including reliability," IEEE Transactions on Power Electronics, vol. 28, no. 1, pp. 325-335, 2013.
12. H. Helali, D. Bergogne, J.B.H. Slama, H. Morel, P. Bevilacqua, B. Allard and O. Brevet, "Power converter's optimisation and design. Discrete cost function with genetic based algorithms," 2005 European Conference on Power Electronics and Applications, pp. 1-7, 2005.
13. L. Jourdan, J-L Schanen, J. Roudet, M. Bensaied, K. Segueni, "Design methodology for non insulated DC-DC converter: application to 42V-14V "Powernet"," IEEE 33rd Annual Power Electronics Specialists Conference, vol. 4, pp. 1679-1684, 2002.
14. S. Busquets-Monge, G. Soremekun, E. Hefiz, C. Crebier, S. Ragon, D. Boroyevich, Z. Gurdal, M. Arpilliere and D. K. Lindner, "Power converter design optimization," IEEE Industry Applications Magazine, vol. 10, no. 1, pp 32-38, 2004.
15. E. Koutroulis and K. Kalaitzakis, "Novel battery charging regulation system for photovoltaic applications," IEE Proceedings - Electric Power Applications, vol. 151, no. 2, pp. 191-197, 2004.
16. G. M. Dousoky, E. M. Ahmed and M. Shoyama, "Current-sensorless MPPT with DC-DC boost converter for photovoltaic battery chargers," 2012 IEEE Energy Conversion Congress and Exposition (ECCE), pp. 1607-1614, 2012.
17. R. Yuanheng, X. Ming, J. Zhou and F. C. Lee, "Analytical loss model of power MOSFET," IEEE Transactions on Power Electronics, vol. 21, no. 2, pp. 310-319, 2006.
18. X. Yu and P. Yeaman, "Temperature-related MOSFET power loss modeling and optimization for DC-DC converter," 28th Annual IEEE Applied Power Electronics Conference and Exposition (APEC), pp. 2788-2792, 2013.
19. K. Billings, H. Keith and T. Morey, "Switchmode Power Supply Handbook", McGraw-Hill, 3rd edition, 2011.
20. L. Jinjun, T. G. Wilson, R. C. Wong, R. Wunderlich and F. C. Lee, "A method for inductor core loss estimation in power factor correction applications," 17th Annual IEEE Applied Power Electronics Conference and Exposition (APEC), vol. 1, pp. 439-445, 2002.
21. W. A. Roshen, "A practical, accurate and very general core loss model for nonsinusoidal waveforms," IEEE Transactions on Power Electronics, vol. 22, no. 1, pp. 30-40, 2007.
22. J. Muhlethaler, J. Biela, J. W. Kolar and A. Ecklebe, "Improved core loss calculation for magnetic components employed in power electronic system," 26th Annual IEEE Applied Power Electronics Conference and Exposition (APEC), pp. 1729-1736, 2011.
23. Z. Michalewicz, "Genetic Algorithms + Data Structures = Evolution Programs," New York: Springer-Verlag, 2nd ed., 1994.
24. E. Koutroulis, K. Kalaitzakis and N. C. Voulgaris, "Development of a microcontroller-based, photovoltaic maximum power point tracking control system," IEEE Transactions on Power Electronics, vol. 16, no. 1, pp. 46-54, 2001.